Finding the temperature window for atomic layer deposition of ruthenium metal via efficient phonon calculations

Alexandr Fonari[a,*], Simon D. Elliott[b], Casey N. Brock[a], Yan Li[a], Jacob Gavartin[c], Mathew D. Halls[d]

[a] Schrödinger Inc., New York, NY 10036, United States

[b] Schrödinger GmbH, 63163 Mannheim, Germany

[c] Schrödinger Technologies Ltd, United Kingdom

[d] Schrödinger Inc., San Diego, CA 92121, United States

[*] Corresponding author. E-mail: alexandr.fonari@schrodinger.com. Address: 1540 Broadway, Floor 24, New York, NY 10036, US

Supplementary Information

Section SI-1: Workflow for bulk screening

The first step of the workflow was to compute electronic energies and free energies of bulk solids, reagent gases and by-product gases with the periodic code Quantum ESPRESSO (Table SI-1), so as to obtain reaction free energies (ΔG) of a range of possible bulk-gas reactions under the conditions of interest (Table SI-2). Here, the free energies have been obtained from full phonon calculations, which are relatively quick for these small systems. Nevertheless, an alternative is to neglect bulk phonons and obtain approximate free energy differences from 'rigid' rotations and translations of gas-phase molecules only (section 3.4), which can be justified as long as the energy differences (ΔE) between reactions are large. Either way, computing bulk solids and gases is an efficient way to screen out unlikely processes or mechanisms, reducing the scope of reactions that need to be studied in more detail at the surface.

The crystal structures of the bulk solids Ru (hcp $P6_3/mmc$) and RuO_2 (rutile $P4_2/mnm$) were optimized with the PBE-D3 functional,[1-3] GBRV ultrasoft pseudopotentials [4] and plane wave cutoffs of 40 Ry for wavefunctions and 200 Ry for charge density, with *k*-point grid planes spaced at 0.04/Å for Ru (10×10×6 Monkhorst-Pack mesh) and 0.10/Å for RuO_2 (6×6×8 mesh). The optimized lattice constants were a=b=2.701 Å, c=4.269 Å, α=β=90°, γ=120° for the Ru_2 cell and a=b=4.501 Å, c=3.131 Å, α=β=γ=90° for the Ru_2O_4 cell.

Molecular models of the reagent and by-product gases H_2, H_2O, RuO_4 and O_2 were generated within otherwise-empty cubic cells so that periodic images were at least 7 Å apart and the structures were optimized with the same functional, pseudopotentials and plane wave cutoffs as for the bulk, but at the Γ *k*-point only.

Phonon calculations (section 3.2) were performed in order to obtain the zero-point energy and free energy corrections for each bulk and gas-phase species (Table SI-1).

Table SI-1. Total energy, zero point energy and free energy correction from full phonon calculations at different temperatures of bulk and molecular systems.

	***E*, Ry**	***ZPE*, kJ/mol**	**Free energy correction (kJ/mol) at *T* (K) and *P*=1 atm**		
			***T*=0°C**	***T*=150°C**	***T*=300°C**
bulk-Ru, per Ru	-188.700	1.958	-1.313	-3.437	-6.205
bulk-RuO_2, per Ru	-252.498	20.043	-2.829	-8.612	-17.106
$H_{2\ (g)}$	-2.332	25.839	-26.978	-47.183	-68.97
$H_2O_{(g)}$	-34.301	54.685	-41.684	-70.747	-101.671
$RuO_{4\ (g)}$	-316.052	32.869	-63.488	-108.376	-157.839
$O_{2\ (g)}$ triplet	-63.492	9.025	-45.038	-75.180	-106.971

The thermodynamics of possible transformations of solid Ru are considered in Reactions **B1**-**B5** of Table SI-2 and shown in Figure SI-1. The most favorable of these reactions involve oxidation by O_2 (**B1** & **B2**), but O_2 should be excluded from the ALD reactor when attempting to deposit Ru metal. Reaction **B3** is also exoergic, indicating that oxidation of bulk Ru metal by RuO_4 is favorable during exposure to this single precursor, and most likely occurs as well when RuO_4 impinges on a surface where Ru metal is accessible. Bulk oxidation by the H_2O by-product is computed to be endoergic (**B4** & **B5**) and so can be ignored as a potential reaction at the surface.

Table SI-2. Reaction free energies (kJ/mol-Ru) of possible reactions of the bulk solids Ru and RuO_2 and gas-phase precursor RuO_4 at temperature T and P=1 atm using the full phonon free energy correction.

Label	**Reaction**	$\Delta_r E$, **kJ/mol**	$\Delta_r G$, **kJ/mol**		
			***T*=0°C**	***T*=150°C**	***T*=300°C**
B1	$Ru_{(s)} + 2O_2 \rightarrow RuO_{4\,(g)}$	-484.2	-443.4	-425.9	-409.0
B2	$Ru_{(s)} + O_{2\,(g)} \rightarrow RuO_{2\,(s)}$	-401.5	-348.9	-322.4	-296.4
B3	$\frac{1}{2} Ru_{(s)} + \frac{1}{2} RuO_{4\,(g)} \rightarrow RuO_{2\,(s)}$	-318.8	-254.4	-218.9	-183.7
B4	$Ru_{(s)} + 2H_2O_{(g)} \rightarrow RuO_{2\,(s)} + 2H_{2\,(g)}$	184.0	172.3	186.3	198.9
B5	$Ru_{(s)} + 4H_2O_{(g)} \rightarrow RuO_{4\,(g)} + 4H_{2\,(g)}$	686.7	598.9	591.6	581.4
B6	$RuO_{2\,(s)} + 2H_{2\,(g)} \rightarrow Ru_{(s)} + 2H_2O_{(g)}$	-184.0	-172.3	-186.3	-198.9
B7	$RuO_{2\,(s)} + O_{2\,(g)} \rightarrow RuO_{4\,(g)}$	-82.7	-94.5	-103.5	-112.7
B8	$RuO_{2\,(s)} \rightarrow Ru_{(s)} + RuO_{4\,(g)}$	318.8	254.4	218.9	183.7
B9	$RuO_{2\,(s)} \rightarrow Ru_{(s)} + O_{2\,(g)}$	401.5	348.9	322.4	296.4
B10	$RuO_{4\,(g)} + 4H_{2\,(g)} \rightarrow Ru_{(s)} + 4H_2O_{(g)}$	-686.7	-598.9	-591.6	-581.4
B11	$RuO_{4\,(g)} \rightarrow RuO_{2\,(s)} + O_{2\,(g)}$	82.7	94.5	103.5	112.7
B12	$RuO_{4\,(g)} \rightarrow Ru_{(s)} + 2O_{2\,(g)}$	484.2	443.4	425.9	409.0
B13	$RuO_{4\,(g)} + 2H_{2\,(g)} \rightarrow RuO_{2\,(s)} + 2H_2O_{(g)}$	-502.8	-426.6	-405.3	-382.6

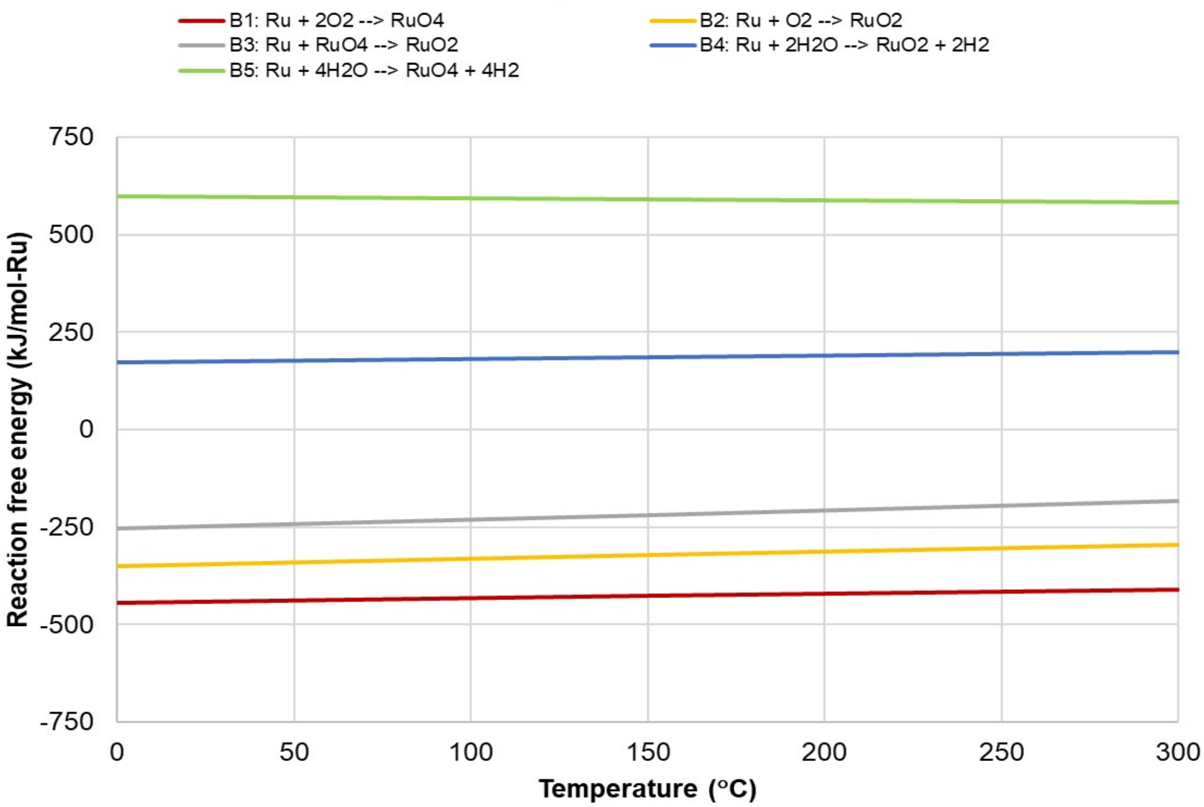

Figure SI-1. Computed free energies from Table SI-2 of potential oxidation reactions of bulk solid Ru with the gases that may be present, namely the precursor RuO_4 and the by-products O_2 and H_2O.

For bulk RuO_2, the negative free energy computed for reduction by H_2 to yield H_2O (reaction **B6**) indicates that this could occur during the H_2 pulse of ALD, and this motivates our study of H_2 reactivity with oxidized Ru surfaces in this paper. The data for reactions **B8** and **B9** show that auto-reduction of RuO_2 in the absence of a reducing agent can not take place.

The reaction for deposition of Ru metal from precursor RuO_4 and co-reagent H_2 (**B10**) is computed to be highly exoergic across the entire temperature range. The competing reaction of oxide deposition (**B13**) is also exoergic. The overall reactions **B10** and **B13** are independent of mechanism, and therefore equally well describe CVD when co-flowing the reagents or ALD from alternating exposures. By contrast, single-source CVD of either RuO_2 or Ru through thermal decomposition of the precursor in the gas phase (reactions **B11** & **B12**) is seen to be endoergic, and can therefore be ignored. However, as noted above, heterogeneous CVD of RuO_2 (reaction

B3) is thermodynamically favorable.

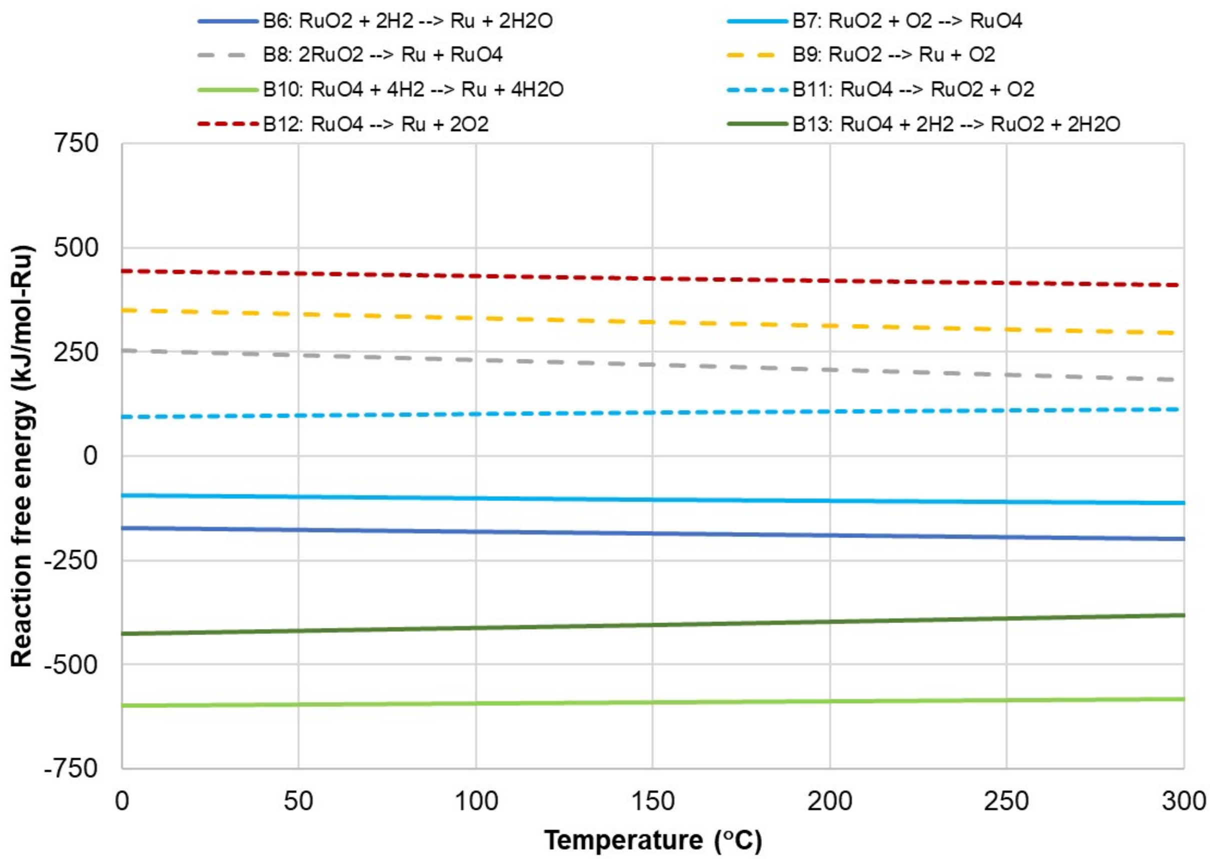

Figure SI-2. Computed free energies from Table SI-2 of potential reactions of bulk solid RuO_2 and of gaseous RuO_4, with dashed lines indicating potential auto-decomposition reactions.

Section SI-2: Workflow for finding saturated surfaces

Saturated surfaces were generated by functionalizing the 2×2 expansion of a bare (0 0 1) Ru slab that is six Ru_4/cell layers thick and separated from images by 10 Å of vacuum. The bare surface is labeled as *.

In order to find a representative structural model of the oxidized surface after the RuO_4 ALD pulse, O atoms were added to one face of the bare slab and the geometry was relaxed with DFT. Coverages ranging 1(O) to 5(O) per Ru_4 cell and on-top, bridging and capping locations were investigated. On-top adsorption, sub-surface positions and peroxide dimers (O-O distance = 1.40 Å) were all found to be less favored energetically than locating O at a capping site, which relaxed to a position equidistant from three surface Ru atoms.

Table SI-3 summarizes the methods used to analyze the total energies of the optimized slabs so as to find the saturating surface. The results presented here are for O_2 gas as oxidant, but equivalent results can be obtained for the ALD precursor RuO_4 as oxidant. As shown in section SI-1, oxidation of bulk Ru by O_2 (or RuO_4) is energetically favorable and so it is not surprising that oxidation of the Ru surface by O_2 at T=0 K and P=1 atm is exoergic overall ($\Delta E_{avg}<0$) for all geometries, albeit decreasing per atom with coverage. More useful is the energy for incremental oxidation by the N^{th} O atom relative to the surface already oxidized by (N-1)O atoms. As shown in Table SI-3, this ΔE_N is negative for $N\leq3$ and positive for $N\geq4$, meaning that oxidation beyond 3(O) per Ru_4 cell is not energetically favorable. An alternative but equivalent approach is to find geometries where surface oxidation is favored relative to bulk oxidation. This is done by viewing the partially-oxidized slabs as mixtures of Ru metal and RuO_2 and computing their surface energies relative to bulk Ru and bulk RuO_2. Using this metric, Table SI-3 again shows that the most stable isomer at coverage of 3(O) per Ru_4 cell has the lowest surface energy, and is thus the saturating surface after oxidation. The structure is shown in Figure SI-3(a). This can be rationalized as the maximum coverage that permits all adsorbed O to occupy hcp capping sites.

The change in ΔE from N=3 to N=4 is so substantial that it is not necessary to adjust for the free energy correction and consider ΔG as a function of temperature for the RuO_4 pulse. However, for the H_2 pulse, it is necessary to compute the temperature-dependent free energy in order to determine which Ru-O-H system is obtained, as various candidate surfaces lie close in energy (section 3 of main paper).

Table SI-3. Analysis of oxidized surfaces, where N is the number of O atoms added per Ru_4 slab, ΔE_{avg} is the oxidation energy relative to O_2 gas averaged over all N(O), ΔE_N is the energy of oxidation by ½O_2 relative to the lowest energy slab with (N-1)O and E_{surf} is the surface energy relative to N/2(bulk-RuO_2) and (24-N/2)(bulk-Ru).

N	**Description of optimized geometry**	**ΔE_{avg} (kJ/mol-O)**	**ΔE_N (kJ/mol-O)**	**E_{surf} (J/m^2)**
1	1(hcp-cap)	-291.5	-291.5	2.84
2	2(hcp-cap)	-257.6	-233.6	2.60
2	1(fcc-cap)+1(sub-layer)	-122.5	+46.5	3.49
3	3(hcp-cap)	-234.9	-189.6	2.47
3	1(hcp-cap)+1(fcc-cap)+1(top)	-209.7	-113.9	2.72
3	3(fcc-cap)	-209.1	-112.1	2.73
4	1(hcp-cap)+1(fcc-cap)+1(sub-layer)+1(bridge)	-144.2	+127.8	3.39
4	1(peroxo)+1(hcp-cap)+1(top)	-134.9	+165.0	3.51
4	1(peroxo)+1(fcc-cap)+1(top)	-125.8	+201.5	3.63
4	4(top)	-103.7	+290.1	3.92
5	1(sub-layer)+1(peroxo)+1(fcc-cap)+1 (bridge)	-98.2	+85.9	4.17
5	2(peroxo)+1(top)	-68.2	+233.4	4.65

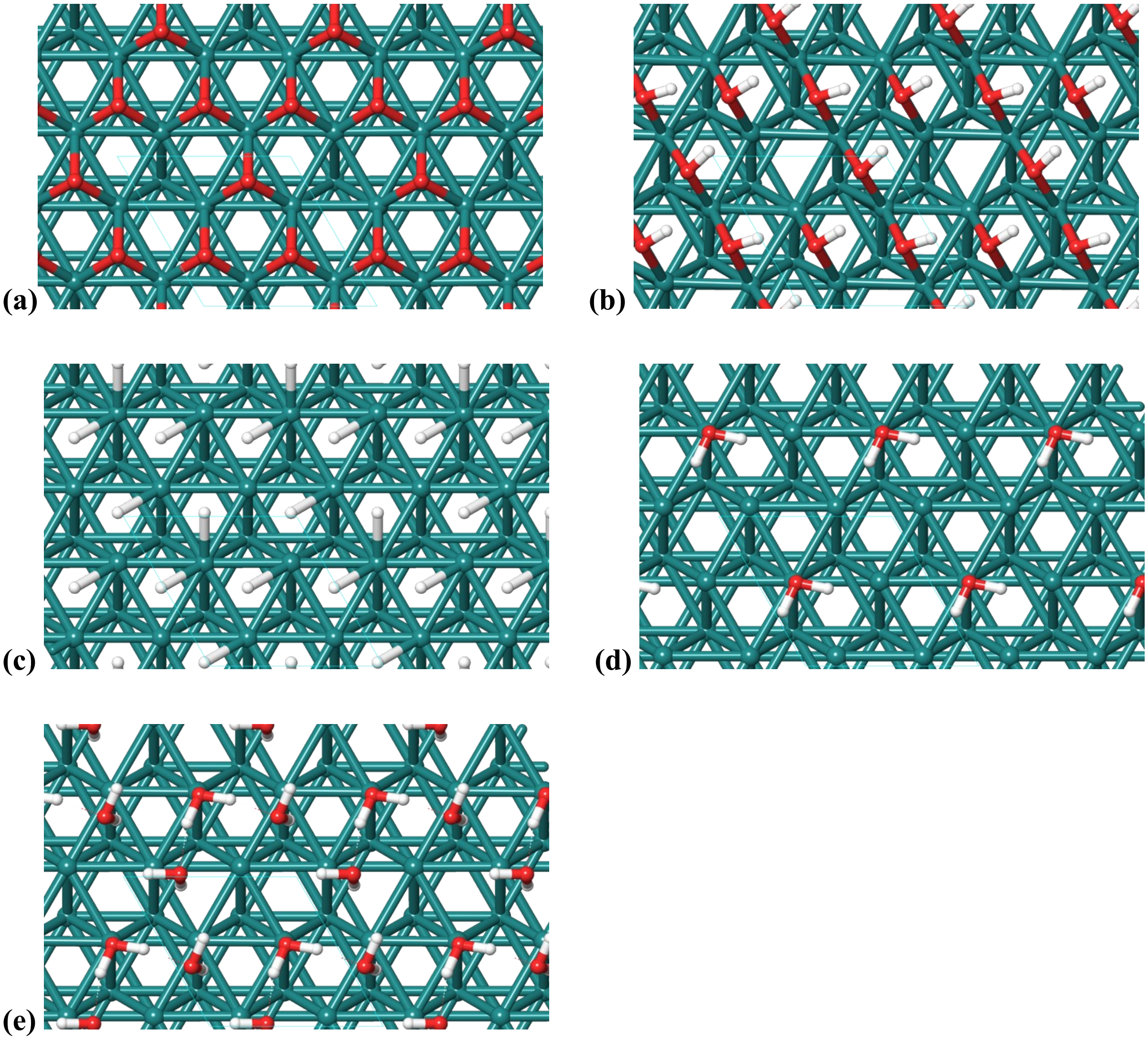

Figure SI-3. Top views of periodic expansions of DFT-optimized slab structures of saturating surfaces and intermediates: (a) [3O]*, (b) [3OH]*, (c) [4H]*, (d) [H_2O]*, (e) [$3H_2O$]*. Ru=turquoise, O=red, H=white. Figure 2 in the main text shows top and side views of a single cell.

Section SI-3: Crossover temperature from rigid approximation

Table SI-4. Gibbs reaction free energies within the rigid approximation ($\Delta_r G^{rigid}$, section 3.4 of main text) over the temperature range of interest and their linear fitting data. Within this approximation *ZPE* is zero. Linear fitting data and zero point energies ($\Delta_r ZPE$) of the Gibbs reaction free energies from full phonon calculations ($\Delta_r G$).

Reaction		$\Delta_r G^{rigid}$ **at *T*, kJ/mol**				$\Delta_r G$**, kJ/mol**	
		0°C	150°C	300°C	Slope, $kJ.mol^{-1}.K^{-1}$	Slope, $kJ.mol^{-1}.K^{-1}$	$\Delta_r ZPE$, kJ/mol
R1	$[3O]^*+3/2H_{2(g)} \rightarrow [3OH]^*$	-7.4	0.1	8.3	0.052	0.040	10.396
R2	$[3O]^*+3H_{2(g)} \rightarrow [3H_2O]^*$	-32.6	-17.5	-1.1	0.105	0.075	20.467
R3	$[3O]^*+3H_{2(g)} \rightarrow [H_2O]^*+2H_2O_{(g)}$	-20.5	-19.8	-18.9	0.005	0.000	15.820
R4	$[3O]^*+3H_{2(g)} \rightarrow * +3H_2O_{(g)}$	-16.9	-23.6	-30.4	-0.045	-0.038	14.223
R5	$[3O]^*+5H_{2(g)} \rightarrow [4H]^*+3H_2O_{(g)}$	-64.1	-60.6	-56.5	0.025	0.030	18.891

Section SI-4: Structure information

System (see Table 1 in the main text for labels): *

```
ATOMIC_POSITIONS crystal
Ru   0.33332193   0.66667876   0.51153846
Ru   0.33332154   0.16667847   0.51153846
Ru   0.16668632   0.33331428   0.05009000   0  0  0
Ru   0.33330956   0.16669048   0.14019600   0  0  0
Ru   0.16667177   0.33332880   0.23385499   0  0  0
Ru   0.33332873   0.16667143   0.32774703   0  0  0
Ru   0.16669104   0.83330982   0.42139905   0  0  0
Ru   0.16669065   0.33330953   0.42139905   0  0  0
Ru   0.16668672   0.83331457   0.05009000   0  0  0
```

```
Ru    0.33330996    0.66669077    0.14019600    0   0   0
Ru    0.16667217    0.83332909    0.23385499    0   0   0
Ru    0.33332913    0.66667172    0.32774703    0   0   0
Ru    0.66669073    0.33330953    0.42139905    0   0   0
Ru    0.83332162    0.16667847    0.51153846
Ru    0.66668641    0.33331428    0.05009000    0   0   0
Ru    0.83330965    0.16669048    0.14019600    0   0   0
Ru    0.66667186    0.33332880    0.23385499    0   0   0
Ru    0.83332882    0.16667143    0.32774703    0   0   0
Ru    0.66669094    0.83330982    0.42139905    0   0   0
Ru    0.83332183    0.66667876    0.51153846
Ru    0.66668662    0.83331457    0.05009000    0   0   0
Ru    0.83330986    0.66669077    0.14019600    0   0   0
Ru    0.66667207    0.83332909    0.23385499    0   0   0
Ru    0.83332903    0.66667172    0.32774703    0   0   0
CELL_PARAMETERS bohr
 10.21002600   0.00000000   0.00000000
 -5.11158200   8.83834600   0.00000000
 -0.00000100   0.00000100  43.09096100
```

System: [3O]*

```
ATOMIC_POSITIONS crystal
Ru    0.17239300    0.33516200    0.42240700    0   0   0
Ru    0.33866400    0.16389700    0.51702100
Ru    0.17391700    0.33470500    0.05143000    0   0   0
Ru    0.33995100    0.16786400    0.14193700    0   0   0
Ru    0.17217000    0.33403500    0.23528600    0   0   0
Ru    0.33997000    0.16750100    0.32833200    0   0   0
O     0.17725600    0.33744400    0.57123000
Ru    0.17433900    0.83598700    0.42411700    0   0   0
```

Ru 0.33860200 0.67250700 0.51704200
Ru 0.17331600 0.83451900 0.05198700 0 0 0
Ru 0.33994700 0.66780400 0.14192000 0 0 0
Ru 0.17357900 0.83490900 0.23615000 0 0 0
Ru 0.34001200 0.66921100 0.32830000 0 0 0
Ru 0.67562800 0.33521200 0.42242400 0 0 0
Ru 0.84136600 0.16951900 0.51862100
Ru 0.67293800 0.33471500 0.05143300 0 0 0
Ru 0.83996900 0.16787400 0.14231500 0 0 0
Ru 0.67410800 0.33401100 0.23528500 0 0 0
Ru 0.84051400 0.16855800 0.33048500 0 0 0
Ru 0.67527200 0.83772700 0.42245300 0 0 0
Ru 0.84707600 0.67238000 0.51704600
Ru 0.67299200 0.83382000 0.05143300 0 0 0
Ru 0.83990200 0.66780200 0.14191300 0 0 0
Ru 0.67416200 0.83609400 0.23523400 0 0 0
Ru 0.84154900 0.66917800 0.32828800 0 0 0
O 0.67387600 0.33751800 0.57129200
O 0.67380500 0.83390800 0.57128500
CELL_PARAMETERS bohr
10.21002600 0.00000000 0.00000000
-5.11158200 8.83834600 0.00000000
-0.00000100 0.00000100 43.09096100

System: [4H]*

ATOMIC_POSITIONS crystal
Ru 0.14717600 0.35670900 0.42189200 0 0 0
Ru 0.31386700 0.19014200 0.51439400
Ru 0.14675900 0.35574100 0.05067100 0 0 0
Ru 0.31357200 0.18948600 0.14111300 0 0 0

```
Ru     0.14732300    0.35645400    0.23464000    0   0   0
Ru     0.31377900    0.18995400    0.32874600    0   0   0
H     0.48042400    0.02339600    0.56045000
Ru     0.14721100    0.85658700    0.42192800    0   0   0
Ru     0.31381800    0.69006700    0.51442400
Ru     0.14682000    0.85579100    0.05072400    0   0   0
Ru     0.31346900    0.68938200    0.14108100    0   0   0
Ru     0.14726500    0.85650000    0.23465000    0   0   0
Ru     0.31389300    0.68997300    0.32873400    0   0   0
H     0.48053600    0.52350000    0.56046100
Ru     0.64731500    0.35670000    0.42189900    0   0   0
Ru     0.81389700    0.19014900    0.51441700
Ru     0.64681500    0.35583900    0.05067600    0   0   0
Ru     0.81361700    0.18939600    0.14109400    0   0   0
Ru     0.64719200    0.35620400    0.23464700    0   0   0
Ru     0.81404400    0.18979700    0.32873400    0   0   0
H     0.98046300    0.02350500    0.56045300
Ru     0.64721100    0.85667700    0.42197600    0   0   0
Ru     0.81390700    0.69008800    0.51442300
Ru     0.64683500    0.85587600    0.05070600    0   0   0
Ru     0.81356200    0.68930700    0.14113000    0   0   0
Ru     0.64717100    0.85620900    0.23462800    0   0   0
Ru     0.81405200    0.68993100    0.32874100    0   0   0
H     0.98043600    0.52350300    0.56048600
CELL_PARAMETERS bohr
 10.21002600   0.00000000   0.00000000
 -5.11158200   8.83834600   0.00000000
 -0.00000100   0.00000100  43.09096100
```

System: [3OH]*

ATOMIC_POSITIONS crystal

Ru	0.11796900	0.30623000	0.42351300	0	0	0
Ru	0.29991100	0.15948600	0.51158500			
Ru	0.12206900	0.30924100	0.05174700	0	0	0
Ru	0.28737600	0.14176800	0.14195000	0	0	0
Ru	0.11991000	0.30777200	0.23548900	0	0	0
Ru	0.28658300	0.14069500	0.32902900	0	0	0
O	0.29375400	0.39516100	0.59055000			
Ru	0.12784700	0.81146700	0.42420800	0	0	0
Ru	0.29996600	0.63552200	0.51152300			
Ru	0.12030100	0.80833200	0.05178900	0	0	0
Ru	0.28748900	0.64192200	0.14193800	0	0	0
Ru	0.11960500	0.80780900	0.23558400	0	0	0
Ru	0.28645200	0.64120800	0.32895900	0	0	0
Ru	0.62993800	0.31393300	0.42258200	0	0	0
Ru	0.78950900	0.14246900	0.51683000			
Ru	0.62230000	0.30945200	0.05136100	0	0	0
Ru	0.78769900	0.14208500	0.14209500	0	0	0
Ru	0.62128100	0.30865400	0.23516500	0	0	0
Ru	0.78571500	0.14036900	0.32961400	0	0	0
Ru	0.63005500	0.81059500	0.42254300	0	0	0
Ru	0.81676600	0.65597500	0.51654300			
Ru	0.62225900	0.80920700	0.05137700	0	0	0
Ru	0.78696900	0.64156800	0.14180300	0	0	0
Ru	0.62145100	0.80854300	0.23514100	0	0	0
Ru	0.78889500	0.64206900	0.32919700	0	0	0
O	0.79982800	0.39730700	0.58790200			
O	0.79956700	0.89842200	0.58790500			
H	0.98473700	1.02823000	0.60654000			
H	0.98513100	0.45263900	0.60645800			
H	0.47929500	0.48848100	0.61026000			

CELL_PARAMETERS bohr

10.21002600 0.00000000 0.00000000

-5.11158200 8.83834600 0.00000000

-0.00000100 0.00000100 43.09096100

System: [H_2O]*

ATOMIC_POSITIONS crystal

Ru	0.04593650	0.23350477	0.42479416	0	0	0
Ru	0.21273680	0.06647601	0.51376903			
Ru	0.04536201	0.23274514	0.05275446	0	0	0
Ru	0.21159792	0.06531699	0.14290238	0	0	0
Ru	0.04528892	0.23254885	0.23649923	0	0	0
Ru	0.21083478	0.06527549	0.33042495	0	0	0
O	0.21391017	0.54972300	0.61802617			
Ru	0.04592564	0.73351917	0.42442425	0	0	0
Ru	0.21221968	0.56807411	0.51590495			
Ru	0.04500331	0.73165329	0.05273600	0	0	0
Ru	0.21164760	0.56556509	0.14269184	0	0	0
Ru	0.04523261	0.73201589	0.23651993	0	0	0
Ru	0.21203132	0.56594629	0.33054862	0	0	0
Ru	0.54598101	0.23366448	0.42314844	0	0	0
Ru	0.71200775	0.06663039	0.51377003			
Ru	0.54474322	0.23180032	0.05261456	0	0	0
Ru	0.71165425	0.06545191	0.14296597	0	0	0
Ru	0.54503552	0.23209429	0.23666404	0	0	0
Ru	0.71264808	0.06559108	0.33043433	0	0	0
Ru	0.54630150	0.73379285	0.42440544	0	0	0
Ru	0.71303072	0.56642841	0.51366154			
Ru	0.54450058	0.73179206	0.05276284	0	0	0
Ru	0.71137700	0.56521850	0.14297268	0	0	0

```
Ru     0.54471324    0.73210035    0.23651989    0   0   0
Ru     0.71270811    0.56727170    0.33039557    0   0   0
H     0.37797631    0.52131087    0.62264583
H     0.04683398    0.35919548    0.62290808
CELL_PARAMETERS bohr
 10.21002600   0.00000000   0.00000000
 -5.11158200   8.83834600   0.00000000
 -0.00000100   0.00000100  43.09096100
```

System: [3H_2O]*

```
ATOMIC_POSITIONS crystal
Ru     0.04497867    0.23592809    0.41682140    0   0   0
Ru     0.20909126    0.06880120    0.50747851
Ru     0.04513328    0.23614494    0.04678474    0   0   0
Ru     0.21192455    0.06959170    0.13732648    0   0   0
Ru     0.04523351    0.23591293    0.23102525    0   0   0
Ru     0.21290420    0.06825964    0.32477967    0   0   0
O     0.09394664    0.39746873    0.64877741
Ru     0.04348385    0.73492668    0.41864789    0   0   0
Ru     0.21458178    0.57129644    0.50732226
Ru     0.04446068    0.73574369    0.04700555    0   0   0
Ru     0.21191743    0.56943206    0.13722237    0   0   0
Ru     0.04499418    0.73589761    0.23070327    0   0   0
Ru     0.21292461    0.57099905    0.32463578    0   0   0
Ru     0.54538886    0.23654835    0.41917217    0   0   0
Ru     0.71153558    0.06597378    0.50773590
Ru     0.54579267    0.23692320    0.04703309    0   0   0
Ru     0.71194072    0.06953140    0.13716847    0   0   0
Ru     0.54525228    0.23622531    0.23074243    0   0   0
Ru     0.70960311    0.06815060    0.32467630    0   0   0
```

Ru	0.54619140	0.73495191	0.41907963	0	0	0
Ru	0.71063657	0.56577501	0.51237788			
Ru	0.54578705	0.73556580	0.04704704	0	0	0
Ru	0.71182872	0.56946541	0.13686667	0	0	0
Ru	0.54536365	0.73598292	0.23073840	0	0	0
Ru	0.71146579	0.56884470	0.32470682	0	0	0
H	0.25878770	0.57939190	0.66045595			
H	0.13753361	0.36385076	0.60832405			
O	0.33071308	0.01185120	0.64880534			
H	0.29304202	-0.05974669	0.60784766			
H	0.16155406	0.02129155	0.66020730			
O	0.71352228	0.54470617	0.61057926			
H	0.87447482	0.51778151	0.62424932			
H	0.55043089	0.35959894	0.62460248			

CELL_PARAMETERS bohr

10.21002600	0.00000000	0.00000000
-5.11158200	8.83834600	0.00000000
-0.00000100	0.00000100	43.09096100

References

1. Perdew JP, Burke K, Ernzerhof M. Generalized Gradient Approximation Made Simple. Physical Review Letters. 1996 Oct 28;77(18):3865–8. DOI: 10.1103/PhysRevLett.77.3865.

2. Grimme S, Antony J, Ehrlich S, Krieg H. A consistent and accurate *ab initio* parametrization of density functional dispersion correction (DFT-D) for the 94 elements H-Pu. The Journal of Chemical Physics. 2010 Apr 21;132(15). DOI: 10.1063/1.3382344.

3. Grimme S, Ehrlich S, Goerigk L. Effect of the damping function in dispersion corrected density functional theory. Journal of Computational Chemistry. 2011 May;32(7):1456–65. DOI: 10.1002/jcc.21759.

4. Garrity KF, Bennett JW, Rabe KM, Vanderbilt D. Pseudopotentials for high-throughput DFT calculations. Computational Materials Science. 2014 Jan;81:446–52. DOI: 10.1016/j.commatsci.2013.08.053